PROCEEDINGS, 51st Workshop on Geothermal Reservoir Engineering
Stanford University, Stanford, California, February 9-11, 2026
SGP-TR-230

Optimizing Cluster Spacing in Enhanced Geothermal Systems

Yuhao Ou[1], Somnath Mondal[2], Alexei A. Savitski[3] and Mukul M. Sharma[1]

[1]The University of Texas at Austin,
Hildebrand Department of Petroleum and Geosystems Engineering

[2]Shell International Exploration and Production Inc, Houston, TX 77082

[3]Shell Exploration & Production Company, Houston, TX 77079

Yuhao199704@utexas.edu

Keywords: Enhanced Geothermal System, Utah FORGE, Project Cape, Heat Recovery, Cluster Spacing, Sensitivity Analysis

ABSTRACT

The economic viability of Enhanced Geothermal Systems (EGS) is fundamentally governed by the balance between thermal energy recovery and the associated costs of subsurface engineering and sustained surface injection. This study conducts a comprehensive numerical investigation to evaluate the thermal performance of a field-scale EGS fluid circulation system. Geologic and well completion data from DOE's Utah FORGE and Fervo's EGS wells in Milford Valley, Utah is used as an example case. A fully coupled hydro-thermal simulator was employed, integrating reservoir, fracture, and wellbore domains to model long-term fluid circulation involving two injection wells and one production well. Sensitivity analyses were performed to assess the impact of key subsurface and operational parameters, including fracture permeability distribution, proportion and spatial arrangement of active fractures, injection rate, inter-well spacing, and cluster spacing. Simulation results highlight that achieving high energy recovery rates in EGS requires strong inter-well hydraulic connectivity and a uniform distribution of fracture permeability. Furthermore, cluster spacing emerges as a critical design parameter, as it governs the trade-off between effective subsurface thermal sweep and surface injection load. To maximize the heat recovery over time, the cluster spacing, and the injection rate can be optimized for a given well spacing. This relationship between these three operator-controlled variables is explored in detail. It is found that for a given well spacing, the optimum cluster spacing increases with the total injection rate. The overall injection rate must be maintained as high as possible but is limited by the fracture propagation pressure (minimum in-situ stress) and the parasitic energy losses needed to pump the fluid. Under these constraints an optimum cluster spacing can be obtained that will maximize the heat recovery rate. These findings provide valuable insights into optimizing EGS design to maximize net energy output and project profitability.

1. INTRODUCTION

This paper presents a synthesis of sensitivity simulations performed for a representative EGS well triplet located at Milford Valley, Utah using published geologic and well completion data from Utah FORGE and Fervo's Project Cape. The goals are to (1) summarize the site context and the modeling framework used to represent a field-scale EGS triplet, (2) quantify how key uncertain or controllable parameters influence long-term heat recovery and injection requirements, and (3) emphasize the role of cluster spacing and active-fracture distribution in controlling thermal sweep efficiency. While multiple parameters are explored, the discussion is organized around completion spacing and flow-path activation, since these variables strongly influence both thermal sustainability and surface injection load.

1.1 Project Cape Overview

Project Cape is an EGS development in southern Utah, positioned near the Utah FORGE research area. The development concept targets crystalline basement rock at depths where fluid temperatures are high enough to support efficient Organic Rankine Cycle (ORC) power conversion. A vertical observation well (Delano 1-OB) was drilled to approximately 9,824 ft to verify the temperature gradient, characterize lithology, and host downhole monitoring equipment including distributed temperature and acoustic sensing. The maximum recorded temperature in the observation well was 444 °F, confirming a high-quality resource (Norbeck et al., 2024).

1.2 Fracture and Cluster Spacing in Multistage EGS

The idea of using horizontal wells with many transverse fractures in EGS has been discussed for more than a decade, drawing directly on the staged-stimulation workflow developed in unconventional oil and gas. Shiozawa and McClure (2014) argued that zonal isolation, multiple stages, and proppant can dramatically improve injectivity/productivity compared with single-stage open-hole stimulation, in part by creating a more uniformly distributed set of flow paths.

Li et al. (2016) performed thermal-breakthrough and rate-constraint calculations for a conceptual two-horizontal-well EGS with multiple stages. Their results highlight that more stages can delay thermal breakthroughs and allow higher circulation rates, but also that maximizing flow rate may be below the maximum achievable rate when thermal decline is a limiting factor. Similarly, Pollack and Mukerji (2018) used Monte-Carlo optimization under geological and stimulation uncertainty and found that fracture spacing is a key decision variable in maximizing discounted project value.

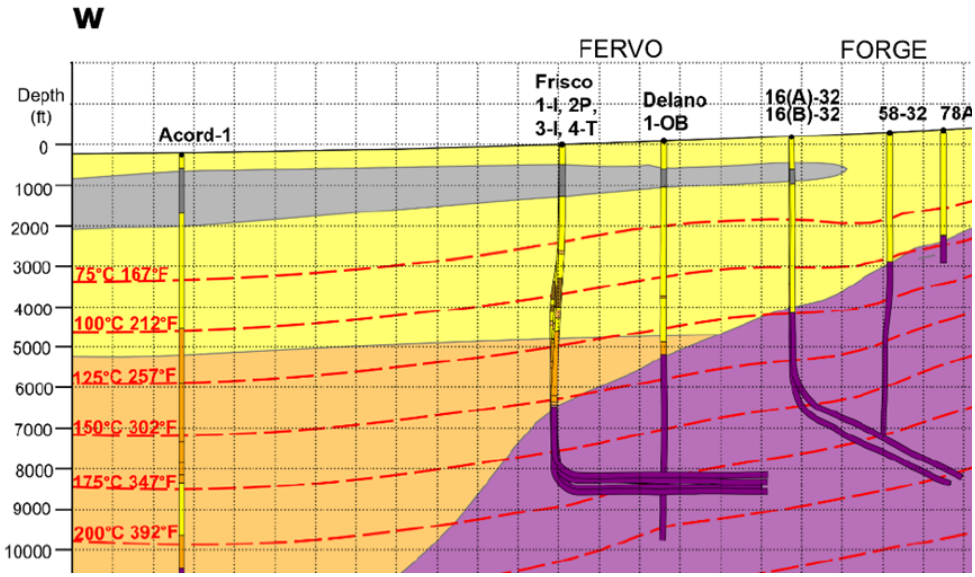

Figure 1: Conceptual cross-section for Project Cape showing the targeted basement interval and temperature isotherms (adapted from Norbeck et al., 2024).

For Project Cape specifically, integrated hydraulic-fracturing and reservoir simulations have been used to evaluate fracturing treatment size and spacing choices prior to drilling and stimulation (Singh et al., 2025). Together, these studies suggest that an optimal cluster or fracture spacing is not universal: it depends on well spacing, injection rate, achievable fracture conductivity, fracture interaction (stress shadow), and economic trade-offs between completion intensity and surface pumping requirements. The present work contributes additional sensitivity results for fracture geometry representing a commercial EGS scale, with particular emphasis on how spacing interacts with flow localization and thermal sweep.

2. MODELING APPROACH AND BASE CASE

2.1 Modeling Concept

To capture the coupled thermo-hydraulic behavior of a multi-stage EGS, we employ a multi-domain numerical model that simultaneously resolves flow and heat transport in three interacting domains: (i) the 3D porous-rock reservoir, (ii) a set of hydraulically stimulated fractures represented as 2D high-transmissivity planes, and (iii) the wellbore network modeled as a 1D conduit from wellhead to each open cluster. The implementation is consistent with integrated reservoir–fracture–wellbore simulators described by Zheng et al. (2020) and Zheng et al. (2021).

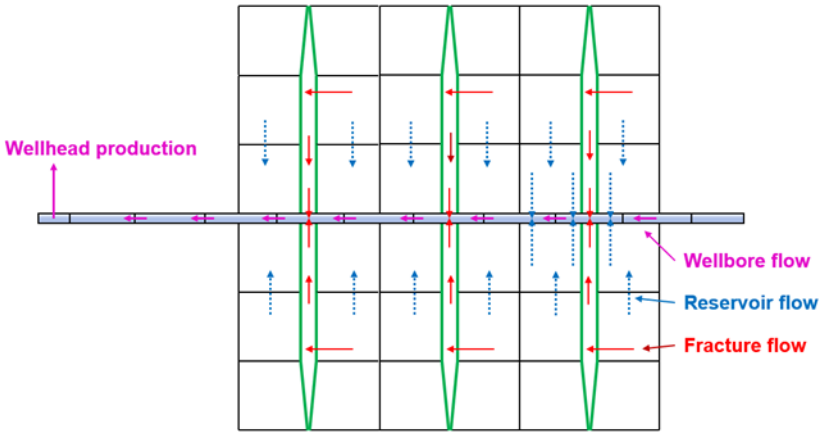

Figure 2: Schematic illustration of the coupled reservoir–fracture–wellbore simulation framework used in this study.

To study long-term heat recovery trends while keeping computational cost manageable, we used a representative field-scale hydro-thermal model of a Cape-like triplet. The model represents one production well centered between two injectors, with multiple transverse hydraulic fractures extending from the wells into a low-permeability host rock. The completion is represented by discrete clusters (or fractures) along the stimulated interval. Cluster spacing is defined as the distance between adjacent fractures along the lateral. Changing the cluster spacing therefore changes the number of fractures and the flow rate allocated to each fracture for a fixed total injection rate. A separate

'active fracture' concept is used to represent imperfect hydraulic connectivity: only a fraction of fractures is assumed to effectively participate in flow to the producer.

2.2 Base Case Parameters and Operating Conditions

The triplet well placement (two injectors flanking one producer) is aligned with the Project Cape well configuration reported by Srinivasan et al. (2025), while the base fracture dimensions (representative fracture height and propped half-length) are consistent with the design simulations summarized by Singh et al. (2025). To reduce computational cost while retaining representative stage-to-stage interference, we simulate a sector model containing five stages of a 27-stage lateral; the wellbore flow rate is calibrated to represent the full 27 stages when computing frictional pressure losses. Figure 3 summarizes the computational mesh and domain decomposition adopted for the base case. Two injectors (I1, I2) and one producer (P) are discretized from the wellhead to the target stage interval. Within each simulated stage, 10 clusters are represented explicitly, with a cluster spacing of 5 m.

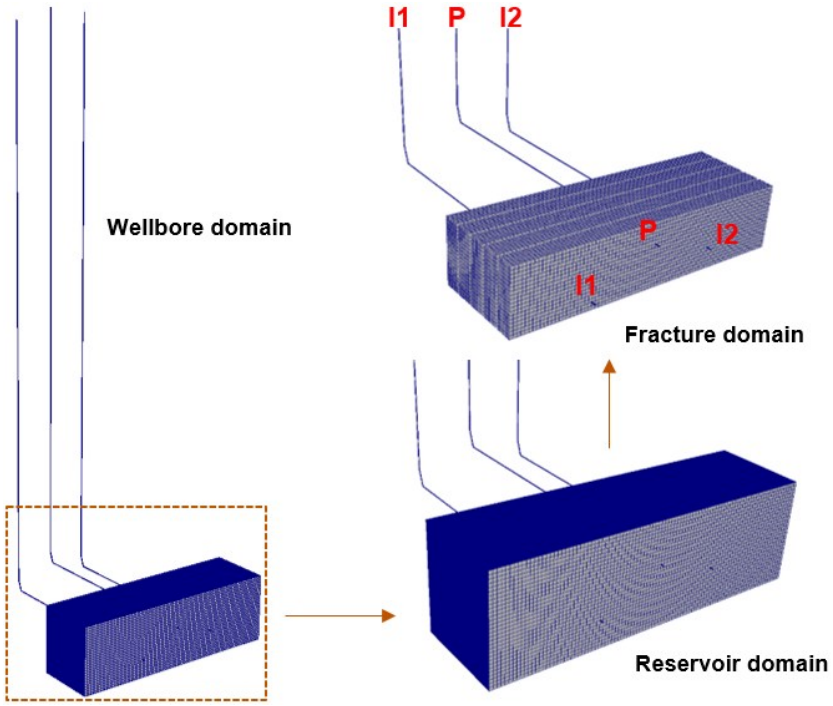

Figure 3: Computational mesh for the base case sector model, illustrating the discretized wellbore, fracture, and reservoir domains.

Table 1: Base case input parameters for the coupled reservoir–fracture–wellbore simulations.

Parameter	Value
Reservoir porosity (%)	2
Reservoir permeability (D)	5e−6
Reservoir pore pressure (Pa)	3e+7
Target formation temperature (°F)	395
Formation compressibility (Pa−1)	1e−9
Water compressibility (Pa−1)	5e−10
Rock heat capacity (J kg−1 K−1)	980
Water heat capacity (J kg−1 K−1)	4200
Water density (kg m−3)	1000
Rock thermal conductivity (W m−1 K−1)	3

Water thermal conductivity (W m−1 K−1)	0.65
Cluster, stage spacing (m)	5, 10
Well spacing (m)	180
Fracture height / half-length (m)	180 / 220
Fracture permeability (D)	24.6
Fracture width (m)	1e−3
Fracture conductivity (md·ft)	80
Fracture injection temperature (°F)	167
Producer WHP (Pa)	2.24e+6

The base case uses uniform fracture conductivity (80 md-ft) for all clusters, assumes all fractures are hydraulically active at the producer, and applies a total injection of 50 kg/s distributed between the two injectors. The nominal well spacing between injector and producer is 180 m, and the base cluster spacing is 5 m. Rock and fluid properties are selected to reflect a hot crystalline reservoir at Cape-like depths, and the injection temperature is held constant for the circulation period.

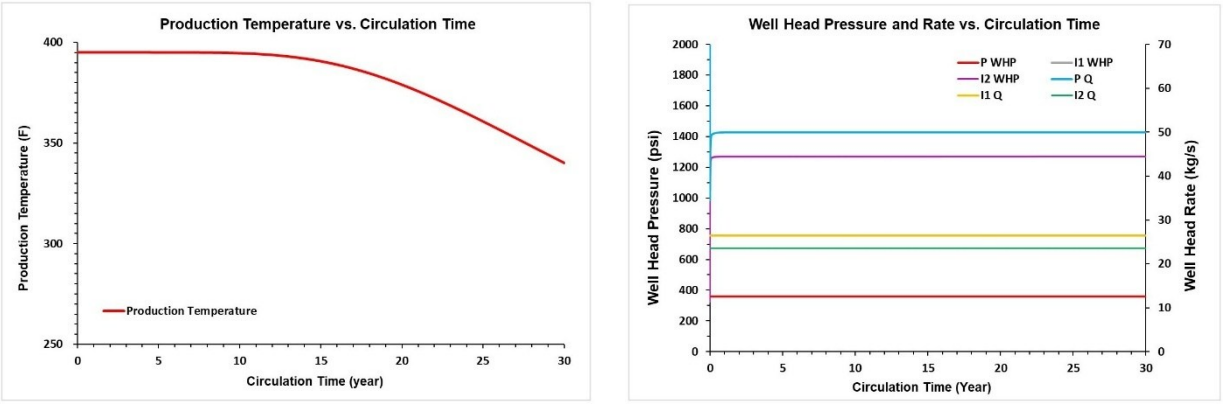

Figure 4: Base case model response: (left) production temperature versus time; (right) wellhead pressures and rates for injectors and producer.

3. SENSITIVITY ANALYSIS DESIGN

A one-factor-at-a-time sensitivity approach was used to isolate how individual parameters affect (1) production temperature (as a proxy for recoverable thermal power) and (2) injector wellhead pressure (as a proxy for surface pumping load and injection feasibility). Table 2 summarizes the simulated cases. Most cases use constant-rate injection.

Table 2: Summary of sensitivity cases.

Case	Change from base case
Base	All fractures active; fracture conductivity 80 md-ft; total injection 50 kg/s; well spacing 180 m; cluster spacing 5 m
1	One fracture 10× conductivity (800 md-ft); others 80 md-ft
2	One fracture 10× conductivity (800 md-ft); others 0.1× (8 md-ft)
3	Normal distribution of fracture conductivity with mean 80 md-ft
4	Only 50% of fractures active at producer (random/nominal distribution)
4a	50% active at producer; active clusters distributed along lateral (c1–c3–c5–c7–c9 pattern)

4b	50% active at producer; active clusters concentrated (c1–c2–c3–c4–c5 pattern)
5	Only 80% of fractures active at producer
6	Well spacing increased to 270 m
7	Well spacing reduced to 90 m
10	Matrix permeability reduced to 5×10^{-7} D
11	Matrix permeability reduced to 5×10^{-8} D
12	Total injection increased to 100 kg/s
13	Total injection increased to 200 kg/s
14	Cluster spacing increased to 10 m
15	Cluster spacing increased to 25 m

4. RESULTS AND DISCUSSION

4.1 Fracture Conductivity Variability and Flow Localization

In the model, conductivity variability is represented either by assigning one fracture a markedly higher conductivity than the rest, or by drawing conductivities from a statistical distribution. The resulting production-temperature and injection-pressure trends (Figure 5) illustrate the sensitivity of thermal lifetime to preferential-flow pathways.

When a single fracture is assigned very high conductivity, a disproportionate fraction of the injected fluid is routed through that pathway. This channeling reduces the effective heat-exchange area and accelerates cooling in the dominant fracture, producing earlier thermal drawdown at the producer. The result reinforces a well-known EGS risk: even if overall transmissivity is high, strong flow localization can shorten the useful life of the system unless completion and stimulation design promote more uniform flow partitioning.

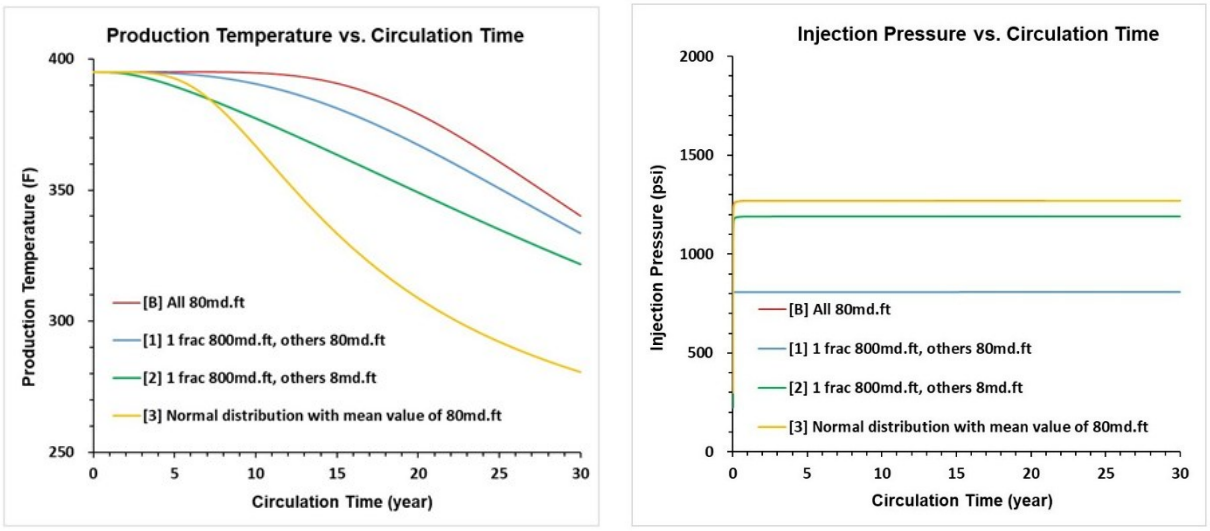

Figure 5: Sensitivity to fracture-conductivity distribution: (left) production temperature versus time; (right) injector wellhead pressure versus time.

4.2 Active-Fracture Fraction and Spatial Arrangement

Not all clusters created during stimulation necessarily contribute equally during long-term circulation. Some fractures may not connect to the producer, may close, or may be bypassed by dominant pathways. To represent this uncertainty, the sensitivity study varies the fraction of 'active' fractures that participate in flow to the producer. Figure 6 shows that reducing the active fraction leads to higher injection pressure (less total flow area) and earlier production-temperature decline (greater flow concentration in the remaining pathways).

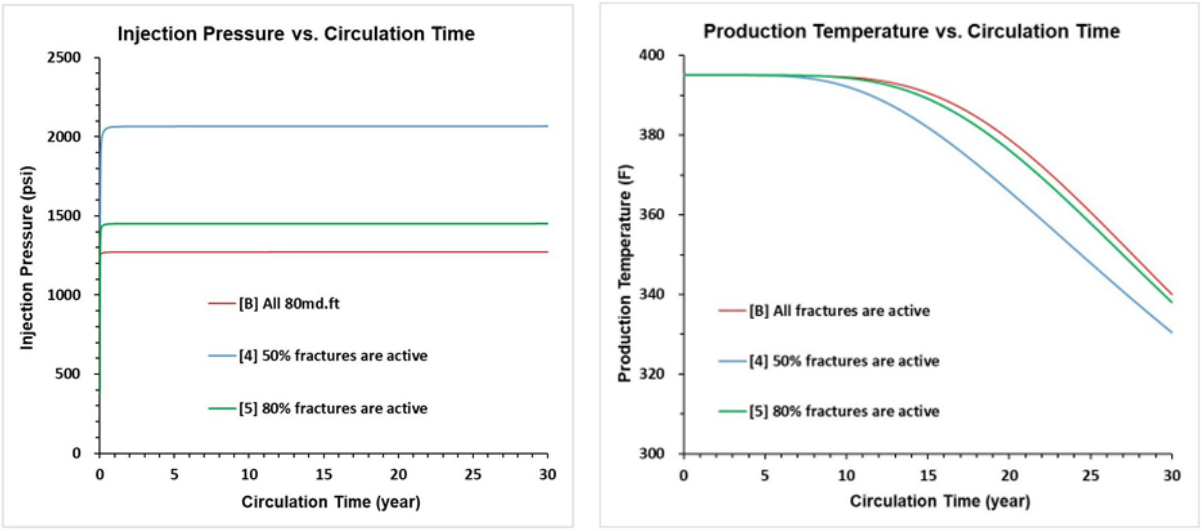

Figure 6: Sensitivity to the fraction of active fractures at the producer: (left) injector wellhead pressure versus time; (right) production temperature versus time.

4.3 Well Spacing

Well spacing controls the characteristic flow-path length between injectors and producer and therefore sets an upper bound on thermal lifetime for a given circulation rate. Increasing the injector-producer spacing increases the contacted rock volume and delays thermal breakthrough, but it also increases hydraulic resistance and can raise required injection pressure. The modeled system exhibits these expected trade-offs. Larger spacing maintains higher production temperature for longer, whereas tighter spacing produces a faster temperature decline.

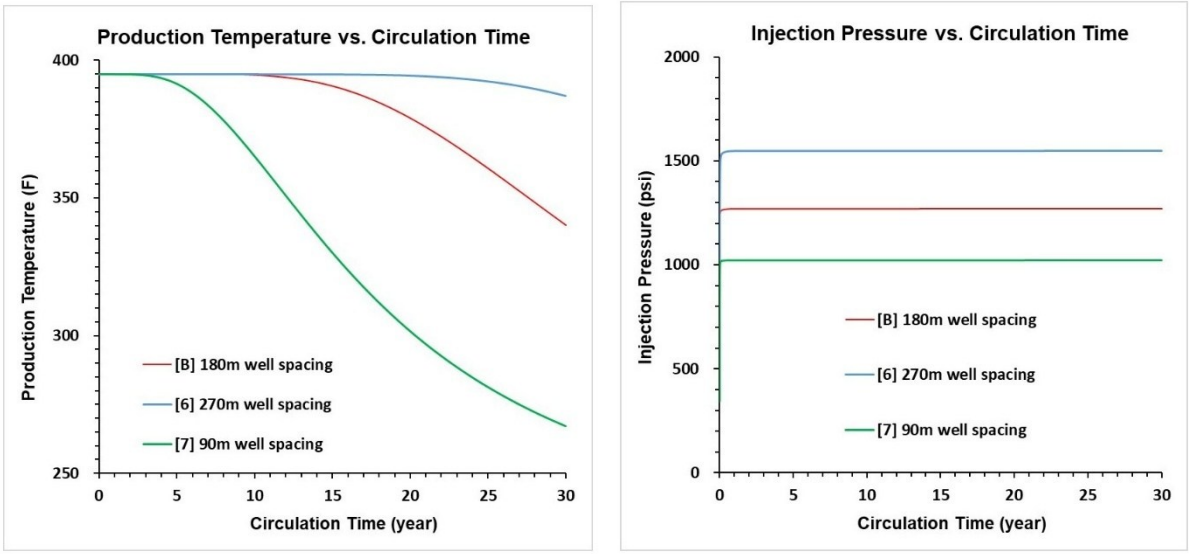

Figure 7: Sensitivity to injector-producer spacing: (left) production temperature versus time; (right) injector wellhead pressure versus time.

4.4 Total Injection Rate

Injection rate influences both the thermal drawdown rate and the surface energy required to circulate fluid. Higher circulation rates increase near-term heat production, but they also accelerate the advance of the cooled zone and can increase wellhead injection pressure due to higher frictional losses in the wellbore and fractures.

Figure 8 illustrates that increasing total injection rate produces earlier temperature decline in the modeled system. This highlights a fundamental design choice for EGS projects: maximizing early-time power output may not maximize long-term cumulative energy recovery unless spacing and completion intensity are adjusted to increase effective heat-transfer area.

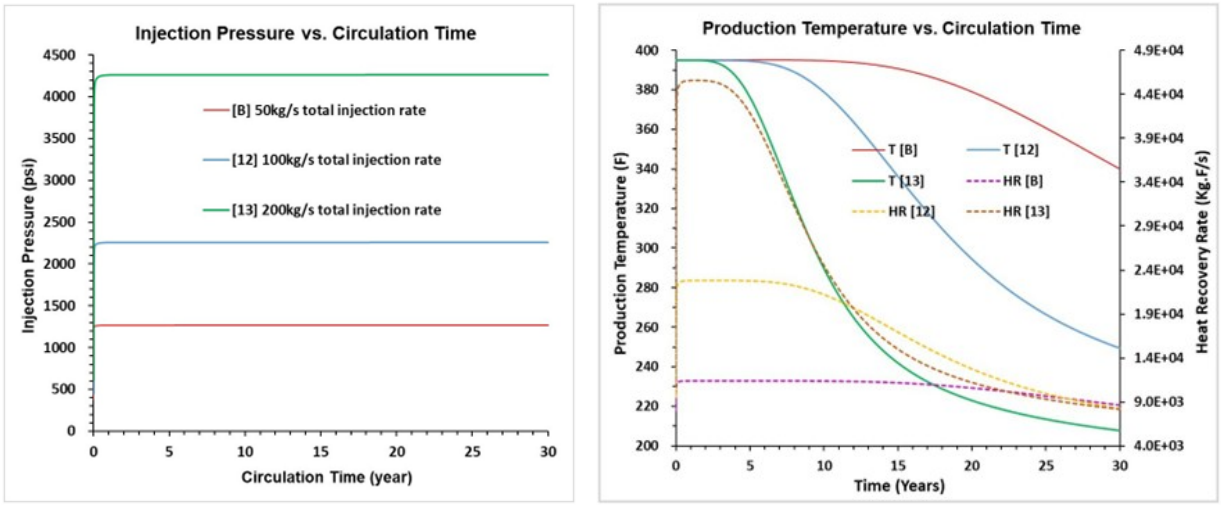

Figure 8: Sensitivity to total injection rate: (left) injector wellhead pressure versus time; (right) production temperature versus time (with heat-recovery rate).

4.5 Cluster Spacing

Cluster spacing directly changes the number of stimulated fractures along the lateral and therefore the per-fracture flow rate for a fixed total injection. In an idealized setting with identical fractures, smaller spacing increases the available flow area, reduces injection pressure, and promotes a more spatially uniform exchange of heat between the circulating fluid and the rock. However, in practice, spacing is also constrained by completion cost, operational complexity, and mechanical fracture interaction (stress shadow), which can reduce stimulation effectiveness when clusters are too closely spaced.

In the Cape-like sensitivity model, increasing cluster spacing from 5 m (base) to 10 m and 25 m produces measurable changes in both injection pressure and thermal drawdown behavior (Figure 9). Wider spacing concentrates more flow into fewer fractures, increasing the likelihood of localized cooling and earlier temperature decline at the producer.

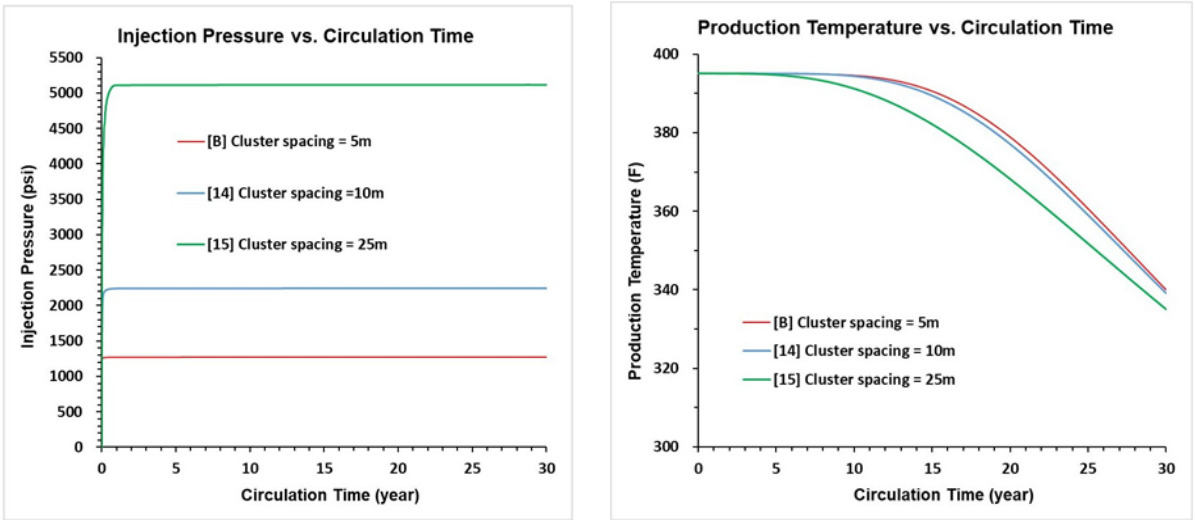

Figure 9: Sensitivity to cluster spacing: (left) injector wellhead pressure versus time; (right) production temperature versus time.

4.6 Improving Cluster Spacing

To strengthen the cluster-spacing narrative, we created an additional case set that isolates completion spacing effects and clarifies the role of effective spacing created by non-uniform cluster activation. The cases (A–F) are summarized in Table 3 and are designed to compare: (1) different spatial distributions of hydraulically active clusters for the same overall active fraction; (2) changes in nominal cluster spacing (10 m vs. 25 m) under otherwise comparable conditions.

Figure 10 summarizes production-temperature decline for Cases A–F. Because Cases A–C share the same nominal 5 m cluster spacing but differ only in which clusters are hydraulically active, their differences reflect the impact of effective spacing and along-well non-uniformity created by incomplete connectivity.

Table 3: Summary of varying cluster spacing cases.

Case	Nominal cluster spacing	Active fraction / pattern	Total injection rate	Notes
Base	5 m	100% active	50 kg/s	Reference completion used in main sensitivities
A	5 m	50% active; c1–c2–c3–c4–c5 (clustered)	50 kg/s	Strongly non-uniform effective spacing
B	5 m	50% active; c1–c3–c5–c7–c9 (alternating)	50 kg/s	Uniform effective spacing ≈ 10 m
C	5 m	50% active; c1–c2–c3–c4–c8 (uneven)	50 kg/s	Intermediate non-uniformity
D	5 m	100% active	100 kg/s	Higher-rate
E	10 m	100% active	50 kg/s	Nominal 10 m spacing; expected to resemble Case B
F	25 m	100% active	50 kg/s	Sparse completion

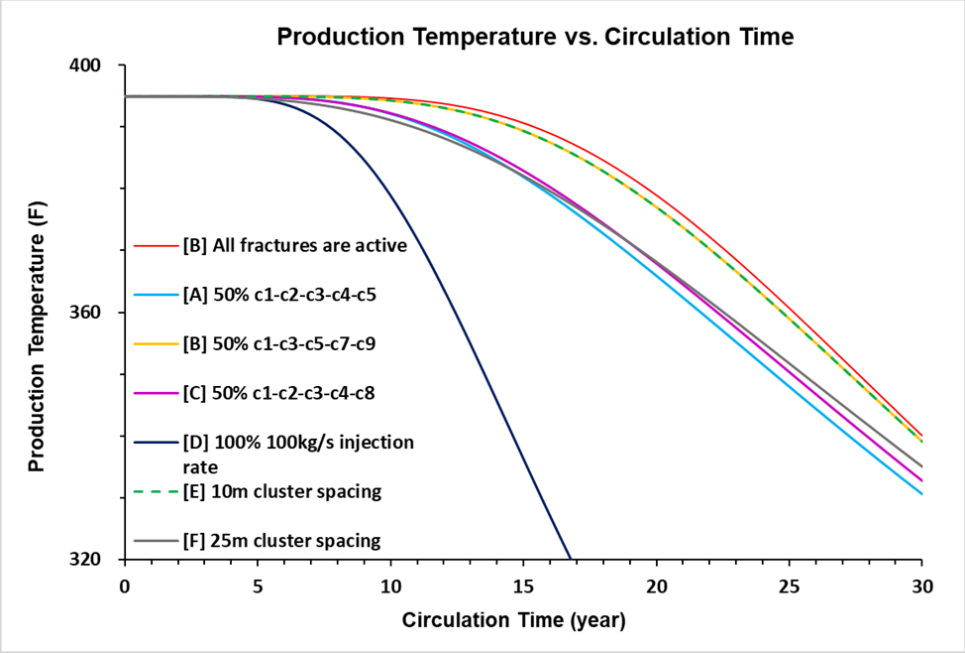

Figure 10: Production temperature versus circulation time for the focused cluster-spacing case set (A–F).

To connect the production-temperature trends in Figure 10 to sweep behavior, Figures 11–12 compare reservoir temperature fields for different active-cluster distributions at the same nominal 5 m completion spacing (Cases A–C). Case B activates every other cluster (c1–c3–c5–c7–c9), producing a nearly uniform effective active spacing of 10 m along the lateral and a relatively continuous cooled corridor. In contrast, Case A concentrates the active clusters in one segment (c1–c5), leaving a long inactive interval; this configuration promotes flow localization and produces a strongly non-uniform cooled zone along the wellbore. Case C is intermediate, where uneven activation produces partial localization but less extreme than Case A. Collectively, these comparisons show that active flow-path spacing can differ substantially from the original completion spacing and can dominate early sweep uniformity.

Cluster spacing and injection rate are coupled through the per-fracture flowrate. For a fixed stimulated lateral length and fixed fracture geometry, the number of active fractures N_{active} scales approximately with effective spacing s_{eff}(i.e., $N_{\text{active}} \propto 1/s_{\text{eff}}$), and the per-fracture flowrate is $q_f = Q_{\text{total}}/N_{\text{active}}$. Thus, changing spacing (or activation) simultaneously changes: (1) how much flow each fracture carries and (2) how much rock volume and heat capacity is available per fracture (and how quickly neighboring cooled zones overlap). The net thermal outcome reflects the competition between these two effects.

Case D (5 m, 100 kg/s) and Case E (10 m, 50 kg/s) can have the same q_f because Case D has roughly twice as many active fractures (denser spacing) while also injecting twice the total mass, shown in Figures 13–16. However, Case D cools substantially faster because the total heat extraction rate is higher (larger Q_{total}) while the available stimulated rock volume is fixed in the model. Equivalently, the denser fracture network in Case D partitions the reservoir into smaller "thermal slices" per fracture and increases fracture-fracture interference, so cooled zones overlap sooner and the lateral-scale temperature decline accelerates. In Case E, the wider spacing provides a larger surrounding rock region per fracture and reduces interference between neighboring cooled zones, so the system better sustains production temperature even at comparable q_f.

Case F (25 m, 50 kg/s) further illustrates the trade-off. Compared with Case E, the much wider spacing increases q_f substantially, which promotes localized cooling "fingers" and reduces sweep efficiency. At the same time, the larger rock region per fracture and reduced interference partially compensates for that higher q_f. As a result, Case F is worse than Case E but can remain better than Case D, where the combination of higher total circulation and denser fracture spacing drives faster system-wide cooling.

Overall, the focused case set shows that cluster spacing is not a purely logistical completion parameter; it is a first-order control on thermal sweep and thermal decline through its coupled impact on (1) effective spacing / interference and (2) flowrate per fracture, which also links directly to injection feasibility and pressure requirements. In the present model formulation (fixed fracture dimensions and prescribed fracture properties), the results suggest an engineering trade-off: moderate cluster spacing (around 10 meters) can provide near-optimal thermal performance while avoiding the high stimulation intensity of very dense spacing and the high q_f penalties of very sparse spacing.

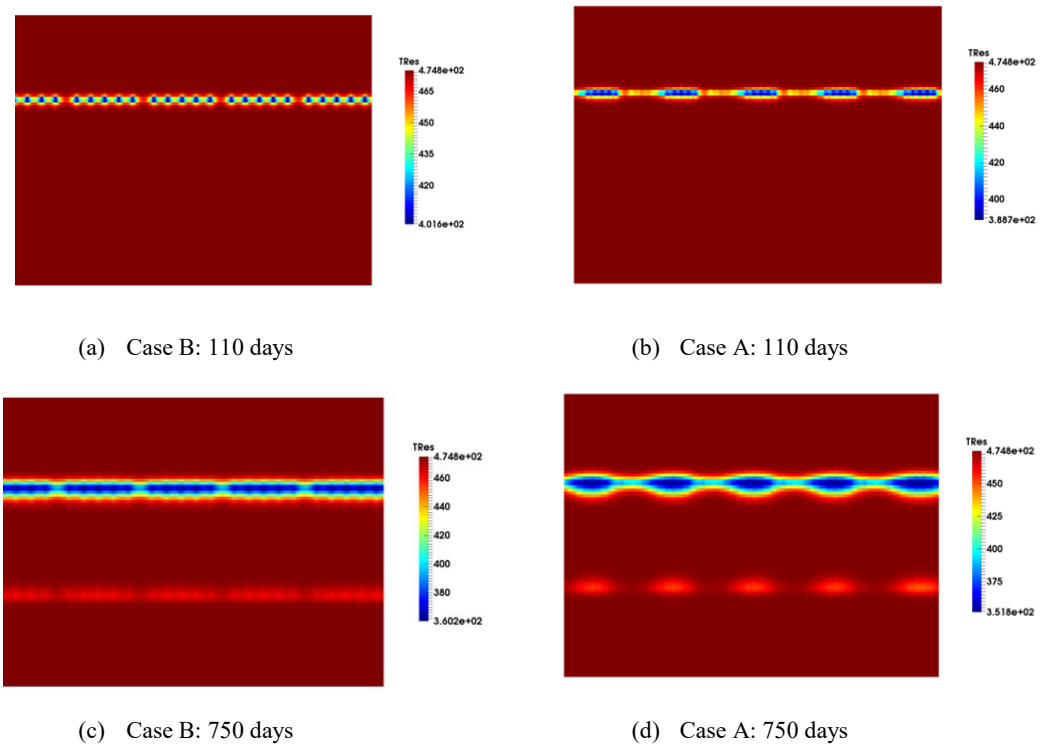

(a) Case B: 110 days

(b) Case A: 110 days

(c) Case B: 750 days

(d) Case A: 750 days

Figure 11: Temperature-field snapshots for Case B (uniform/alternating active clusters; effective spacing ~10 m) versus Case A (clustered active clusters). Early-time behavior (110 and 750 days). Distance between the two injectors is 360 meters.

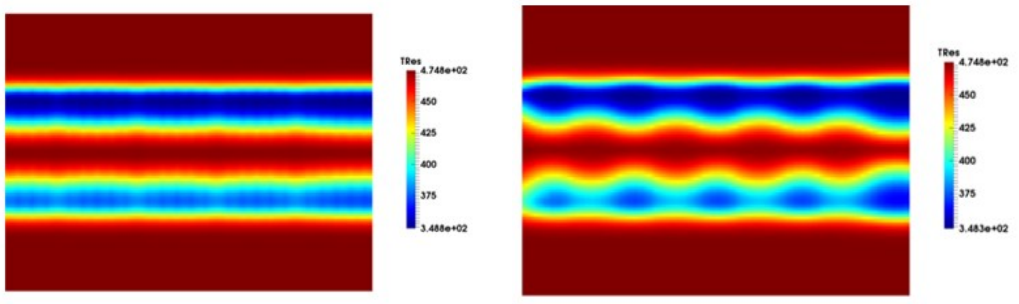

(a) Case B: 15.7 years (b) Case A: 15.7 years

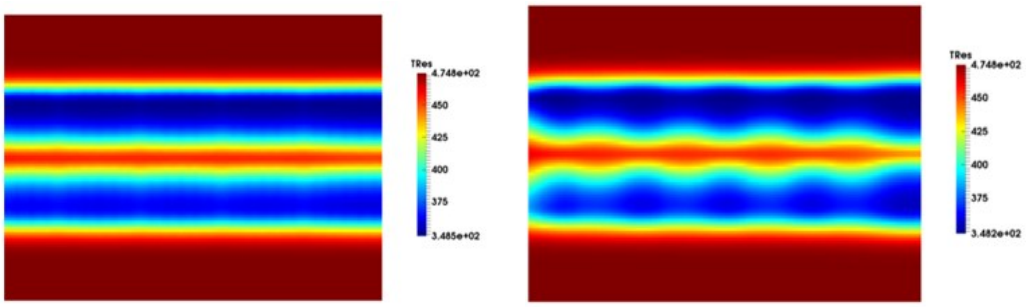

(c) Case B: 30 years (d) Case A: 30 years

Figure 12: Temperature-field snapshots for Case B versus Case A at later times (15.7 and 30 years). Distributed activation maintains a smoother cooled corridor, while clustered activation retains strong along-well non-uniformity. Distance between the two injectors is 360 meters.

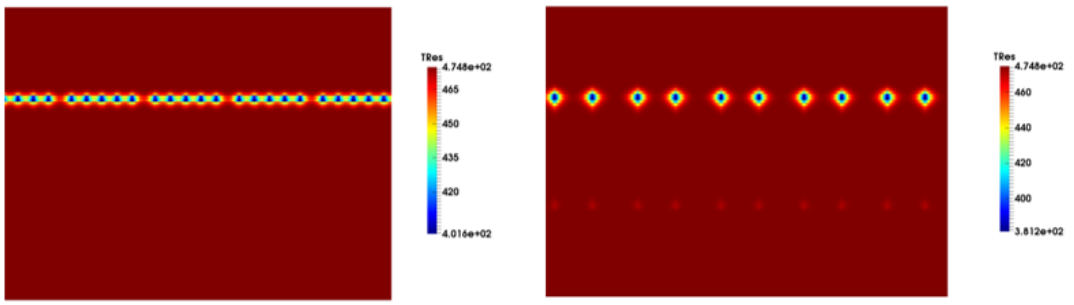

(a) Case E: 110 days (b) Case F: 110 days

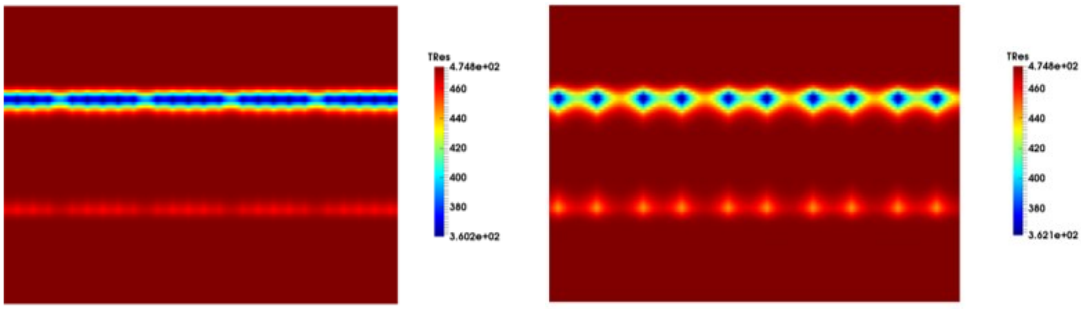

(c) Case E: 750 days (d) Case F: 750 days

Figure 13: Temperature-field snapshots comparing Case E (10 m) and Case F (25 m). Early-time behavior (110 and 750 days). Distance between the two injectors is 360 meters.

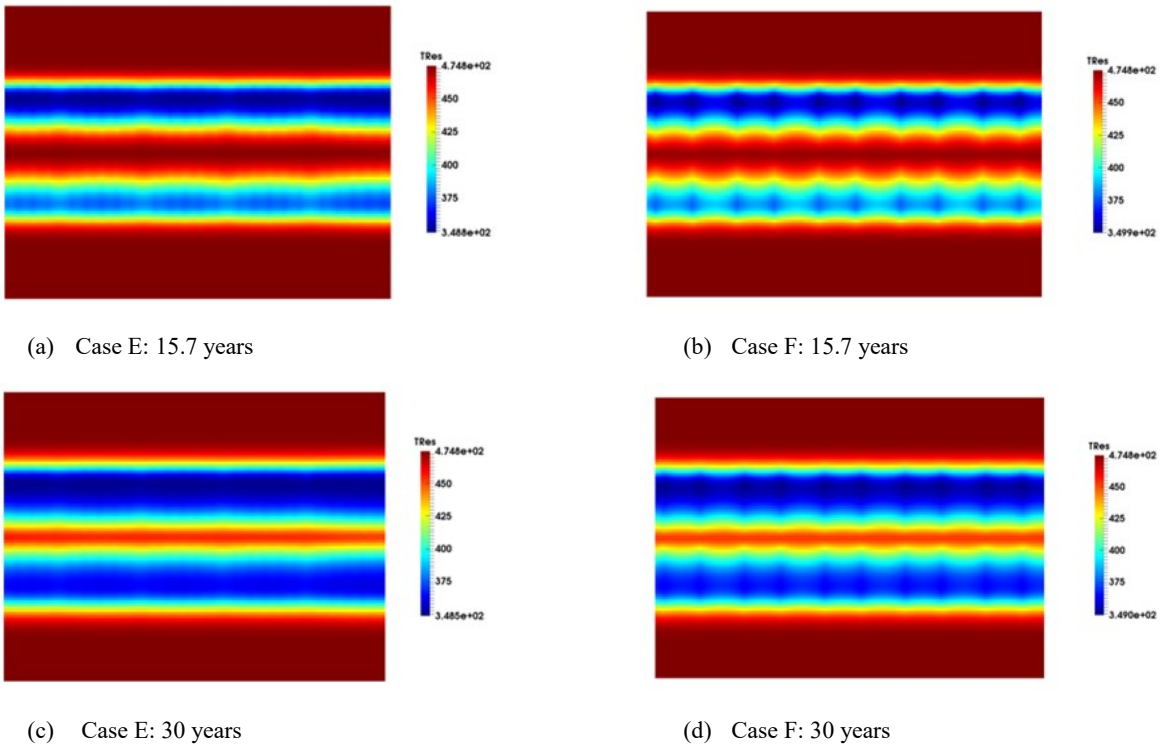

(a) Case E: 15.7 years

(b) Case F: 15.7 years

(c) Case E: 30 years

(d) Case F: 30 years

Figure 14: Temperature-field snapshots comparing Case E (10 m) and Case F (25 m) at later times (15.7 and 30 years). Distance between the two injectors is 360 meters.

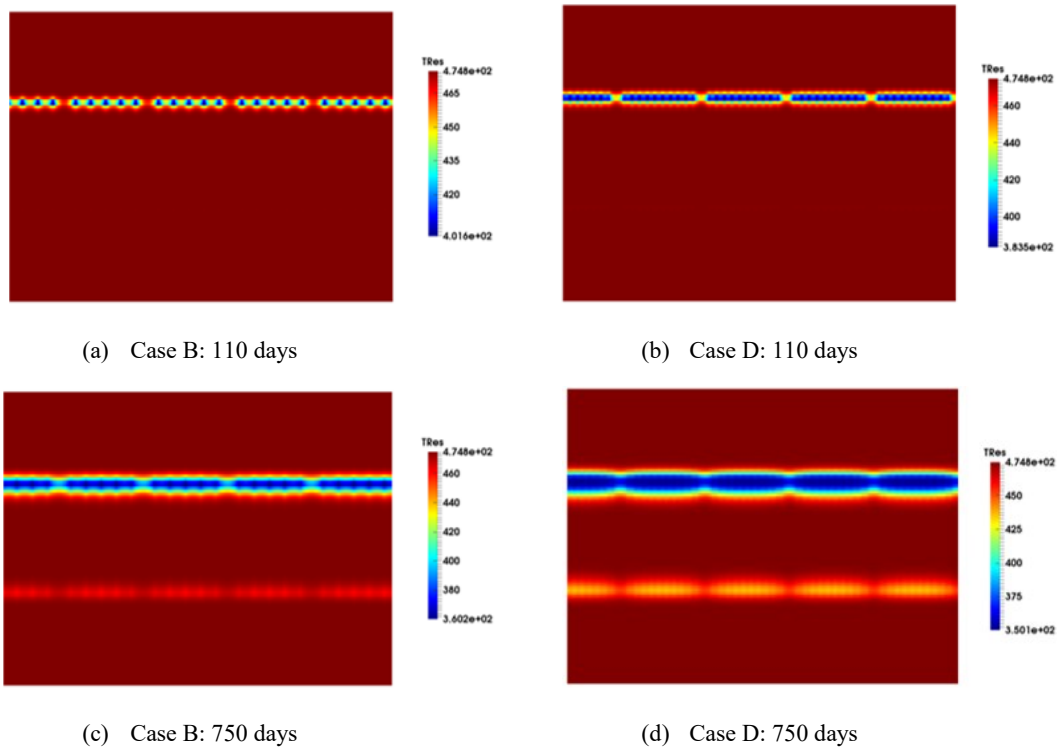

(a) Case B: 110 days

(b) Case D: 110 days

(c) Case B: 750 days

(d) Case D: 750 days

Figure 15: Temperature-field snapshots comparing Case B (effective 10 m spacing) and Case D (100% active, 100 kg/s total injection). Distance between the two injectors is 360 meters.

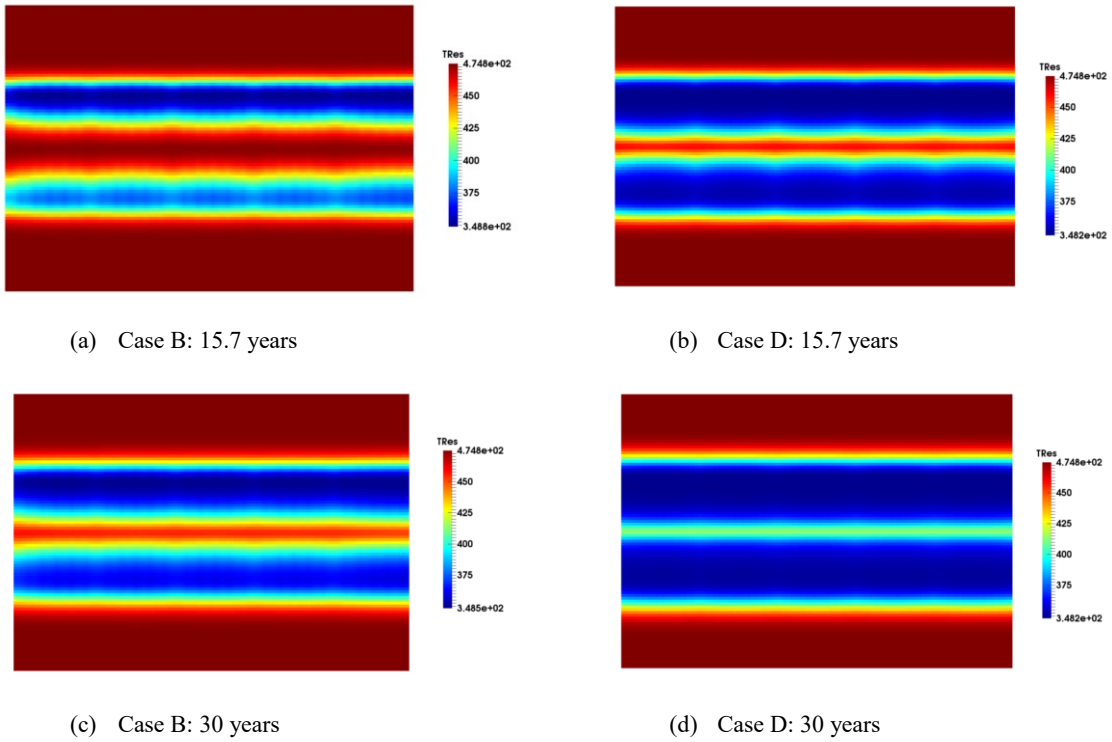

(a) Case B: 15.7 years

(b) Case D: 15.7 years

(c) Case B: 30 years

(d) Case D: 30 years

Figure 16: Temperature-field snapshots comparing Case B (10 m) and Case D (25 m) at later times (15.7 and 30 years). Distance between the two injectors is 360 meters.

5. CONCLUSIONS

1. A field-scale hydro-thermal sensitivity study was summarized for a representative simulation of Project Cape (Milford Valley, Utah), with emphasis on completion spacing and active-fracture connectivity.

2. Fracture-conductivity heterogeneity can cause strong flow localization and earlier thermal drawdown, underscoring the need for completion strategies that promote more uniform flow partitioning.

3. Reducing the fraction of hydraulically active fractures increases injection pressure and accelerates thermal decline. Distributing active clusters more evenly along the lateral improves thermal sweep and reduces along-well temperature non-uniformity.

4. Denser cluster spacing (e.g., 10 m versus 25 m) lowers the mass flow rate per fracture and, therefore, the injection pressure and cools the region between the fractures without causing early breakthrough of the cooled region.

5. However, if the cluster spacing is reduced from 10 m to 5 m, keeping the mass flow rate per fracture the same (doubling the total injection rate), the rock between two adjacent fractures cools much faster. This leads to a rapid advancement of the cooled region towards the producer and an early onset of decline in energy production rate. The energy recovery rate is much higher for the higher mass flow rate, but this leads to a quicker decline rate over time.

6. The optimum cluster spacing balances the higher energy recovery rate achieved with smaller cluster spacing with the higher rate of decline of energy recovery over time. The optimum cluster spacing is primarily a function of the well spacing and the mass injection rate.

7. Economic and mechanical constraints can also influence the optimal cluster spacing, based on completion and stimulation costs..

REFERENCES

Li, T., Shiozawa, S., & McClure, M. W. (2016). Thermal breakthrough calculations to optimize design of a multiple-stage Enhanced Geothermal System. Geothermics, 64, 455–465. https://doi.org/10.1016/j.geothermics.2016.06.015

Norbeck, J., Gradl, C., & Latimer, T. (2024). Deployment of Enhanced Geothermal System technology leads to rapid cost reductions and performance improvements. EarthArXiv preprint.

Pollack, A., & Mukerji, T. (2018). Optimization of Enhanced Geothermal Systems under Geological and Reservoir Stimulation Uncertainty. GRC Transactions, 42.

Shiozawa, S., & McClure, M. W. (2014). EGS designs with horizontal wells, multiple stages, and proppant. Proceedings, 39th Workshop on Geothermal Reservoir Engineering, Stanford University, SGP-TR-202.

Singh, A., Galban, G., McClure, M., Briggs, K., & Norbeck, J. (2025). Designing the Record-Breaking Enhanced Geothermal System at Project Cape. Unconventional Resources Technology Conference (URTeC 4245311). https://doi.org/10.15530/urtec-2025-4245311

Srinivasan, A., Wu, K., Jin, G., Titov, A., & Dadi, S. (2025). Characterizing Fracture Geometry Using Integrated Fiber-Optic Strain Data from Horizontal and Vertical Monitoring Wells: A Case Study in Enhanced Geothermal Systems. Unconventional Resources Technology Conference (URTeC 4258573). https://doi.org/10.15530/urtec-2025-4258573

Tester, J. W., et al. (2006). The Future of Geothermal Energy. Massachusetts Institute of Technology.

U.S. Department of Energy. (2019). GeoVision: Harnessing the Heat Beneath Our Feet. https://doi.org/10.2172/1879171

Zheng, S., & Sharma, M. M. (2020). An Integrated Equation-of-State Compositional Hydraulic Fracturing and Reservoir Simulator. SPE Paper SPE-201700-MS. https://doi.org/10.2118/201700-MS

Zheng, S., Hwang, J., Manchanda, R., & Sharma, M. M. (2021). An integrated model for non-isothermal multi-phase flow, geomechanics and fracture propagation. Journal of Petroleum Science and Engineering, 196, 107716. https://doi.org/10.1016/j.petrol.2020.107716

Zhou, Q., & Chen, B. (2023). Modeling Thermal Fracturing During Operation of Enhanced Geothermal Systems: Improved Heat-Transfer Area and Reservoir Sustainability. Proceedings, 48th Workshop on Geothermal Reservoir Engineering, Stanford University, SGP-TR-224.